Characterization of Bone Tissue and Bone Morphology in Taurine Transporter Knockout Mice

Toshihiro Kato, Ning Ma, Takashi Ito, Akinobu Nishimura, Akihiro Sudo, and Takenori Yamashita

Keywords

Taurine · TauT KO mice · BMD · Bone microstructure

T. Kato
Department of Rehabilitation, Suzuka Kaisei Hospital, Suzuka, Mie, Japan

Department of Orthopaedic and Sports Medicine, Mie University Graduate School of Medicine, Edobashi, Tsu, Mie, Japan

N. Ma · T. Yamashita (✉)
Division of Health Science, Graduate School of Health Science, Suzuka University of Medical Science, Suzuka, Mie, Japan
e-mail: takenori@suzuka-u.ac.jp

T. Ito
Faculty of Biotechnology, Fukui Prefectural University, Fukui, Japan

A. Nishimura
Department of Orthopaedic and Sports Medicine, Mie University Graduate School of Medicine, Edobashi, Tsu, Mie, Japan

A. Sudo
Department of Orthopaedic and Sports Medicine, Mie University Graduate School of Medicine, Edobashi, Tsu, Mie, Japan

Department of Orthopaedic Surgery, Mie University Graduate School of Medicine, Edobashi, Tsu, Mie, Japan

Abbreviations

ALP	Alkaline phosphatase
BMD	Bone mineral density
BS	Bone surface
BV	Bone volume
DEXA	Dual-energy X-ray absorptiometry
TauT	Taurine transporter
Tb.N	Trabecular number
Tb.Sp	Trabecular separation
Tb.Th	Trabecular thickness
TV	Total volume

1 Introduction

Taurine, a sulfur-containing amino acid, has been shown to have multiple functions, including antioxidative and membrane stabilization activities and roles in modulating the cell volume, ion channel activities, and intracellular calcium levels (Pasantes-Morales and Cruz 1985; Gordon et al. 1992; Huxtable 1992; Camerino et al. 2004; Hoffmann et al. 2009; Kato et al. 2015). It is synthesized primarily by the liver and accumulated in various tissues in the body (Moon et al. 2012). Depending on the species, intracellular concentrations of taurine can vary from 10 to 70 mmol/L in the mammalian heart, brain, neutrophils, skeletal muscle, liver, and retina (Suleiman et al. 1997). By contrast, its extracellular concentrations have been shown to reach only 600–

S. W. Schaffer et al. (eds.), *Taurine 12*, Advances in Experimental Medicine and Biology 1370,
https://doi.org/10.1007/978-3-030-93337-1_20

800 nmol/L in mice (Shigemi et al. 2011). This steep taurine concentration gradient between the intracellular and extracellular spaces is built up by a sodium-dependent transport system called the taurine transporter (TauT) (Rasgado-Flores et al. 2012), which is expressed in mammalian tissues. Because the ability to synthesize taurine is limited in most tissues, the maintenance of high intracellular concentrations of this amino acid depends upon its uptake from the extracellular space via TauT (Baliou et al. 2020).

In bone tissue, taurine accounts for 0.1% of the body weight, making it an effective element in the regulation of bone metabolism (Gupta et al. 2005; Jeon et al. 2007). Taurine promotes the differentiation of osteoblasts, which also express TauT to maintain a constant intracellular level of the amino acid (Yuan et al. 2006). This amino acid also mediates the activation of alkaline phosphatase (ALP) activity and osteocalcin secretion and the inhibition of osteoclastogenesis (Yuan et al. 2010). Additionally, taurine affects not only bone remodeling but also the expression of connective tissue growth factor and the synthesis of collagen in osteoblast-like cells (Park et al. 2001; Yuan et al. 2007). Choi (2009) has shown that the oral supplementation of taurine could increase the femur bone mineral content in growing rats and may have positive results on bone metabolism in alcohol-fed ovariectomized rats. However, the long-term administration of taurine may have an adverse effect on the bone microstructure. Because of the sulfur-containing characteristic of taurine, its excessive intake could yield increased sulfuric acid production in the body, whereupon the skeleton may need to act as a buffer to neutralize the excess acid (Martiniakova et al. 2019). The effects of taurine on bone may depend on its dose and the subject's general physical condition.

Previous studies have reported the correlation of severe taurine deficiency with the presentation of a variety of disorders in various tissues (e.g., the eye, kidney, heart, and muscle) of TauT knockout (TauT−/−) mice (Warskulat et al. 2004; Ito et al. 2008). However, the exact effects of taurine deficiency or depletion on bone metabolism and bone quality have not been elucidated. Therefore, our aim in this study was to clarify this by comparing the bone mineral density (BMD) and bone microstructure of TauT−/− and TauT+/+ mice.

2 Methods

2.1 Animals and Chemicals

Male TauT−/− and TauT+/+ mice (20 months old) were obtained by mating heterozygous males and females (Ito et al. 2008). The animals were housed in a specific pathogen-free room kept at 22.0 °C and 45–55% relative humidity, under a 12-h light/dark cycle, and given ad libitum access to water and food (MF, Oriental Yeast, Tokyo, Japan). For each experiment, five animals from each mouse group were euthanized, and their tissues were isolated for study. All animal experimental protocols were conducted in accordance with the Guidelines for the Care and Use of Laboratory Animals and approved by the Animal Ethics Committee of Suzuka University of Medical Science, Suzuka, Mie, Japan.

2.2 Histopathological and Immunohistochemical Studies

For each mouse, the right femur was evaluated for its bone microarchitecture and BMD, whereas the left femur was used to prepare a decalcified section for histomorphometric analysis. The femur bones were fixed with 4% formaldehyde in phosphate-buffered saline for 1 day. Then, after their dehydration and paraffin infiltration, the bones were embedded in paraffin blocks, which were subsequently sectioned to 6 μm thickness using a microtome (Leica Microsystems, Wetzlar, Germany) according to routine protocols. After a 48-h heat treatment at 40 °C, the tissue sections were deparaffinized with xylene, hydrated with a gradient series of alcohol, and then washed once with tap water for 5 min. Thereafter, the sections were boiled in 5% urea for 5 min in a microwave oven (500 W) for antigen retrieval. Following

epitope retrieval, endogenous peroxidases were inactivated by incubating the samples with 1% H_2O_2 at 25 °C for 15 min. Then, after blocking the sections with 1% skimmed milk for 20 min, they were incubated with primary antibodies against TauT (1:200 dilution; cat. no. sc-393036; Santa Cruz Biotechnology Inc., Dallas, TX, USA) at 20 °C overnight, followed by biotinylated secondary antibodies (Vector Laboratories, Burlingame, CA, USA) at 25 °C for 1 h. The immunocomplexes were visualized using the Peroxidase Stain DAB Kit (Nacalai Tesque, Inc., Kyoto, Japan) according to the manufacturer's instructions. The nuclei were counterstained with hematoxylin, and the sections were finally observed and photographed under a microscope (BX53; Olympus, Tokyo, Japan). Immunostaining without primary antibodies was carried out for the negative control sections, which subsequently revealed no positive staining (data not shown).

The histopathological appearance of the bones was evaluated by hematoxylin and eosin staining. The thickness of the femoral growth plate was measured using ImageJ software (version 1.48).

2.3 Measurement of Bone Mineral Density

The BMD of the femur was assessed by dual-energy X-ray absorptiometry (DEXA) using an apparatus for small animals (Dichroma Scan DCS-600; Aloka, Osaka, Japan) according to a previous study. Two femur regions were measured: proximal and mid-diaphysis. The proximal femur represented cancellous bone, whereas the mid-diaphysis of the femur was the cortical bone area.

2.4 Micro-computed Tomography Bone Analysis

The bone microstructure in the proximal femur was assessed by micro-computed tomography (micro-CT) (SMX-90CT; Shimadzu, Kyoto, Japan). Three-dimensional microstructural imaging data were reconstructed, and structural parameters were calculated using TRI/3D-BON software (RATOC System Engineering, Tokyo, Japan). The micro-CT imaging conditions used were as follows: tube current, 110 μA; tube voltage, 90 kV; integration time, 200 ms; and voxel size, 23 μm × 23 μm × 23 μm. The scan was conducted at constant intervals of 23 μm over a region of 920 μm in length from the inferior border of the femur head. The structural parameters measured were the total volume (TV), bone volume (BV), bone surface (BS), bone volume fraction (BV/TV), bone surface to total volume ratio (BS/TV), trabecular thickness (Tb.Th), trabecular number (Tb.N), and trabecular separation (Tb.Sp).

2.5 Statistical Analysis

All data are presented as the mean ± standard deviation. Student's t-test (SPSS 21.0) was used to examine differences between the TauT−/− and TauT+/+ mice. Differences in values were considered statistically significant at $P < 0.05$.

3 Results

3.1 External Appearance, Histopathology, and Immunohistochemistry of the TauT−/− Mouse Femurs

The external appearance of the femurs and histological staining of the tissue are shown in Fig. 1. The femurs of the TauT−/− mice showed normal external morphology and appeared similar to those of the TauT+/+ mice (Fig. 1a). There was also no significant difference in femur length between the TauT−/− and TauT+/+ groups (17.0 ± 0.06 and 17.1 ± 0.12 mm, respectively; $P = 0.563$). The TauT−/− mouse femur had the following specific histological features: (1) a small number of trabeculae, (2) thin cortical bone and epiphyseal plate thicknesses, and (3) a wide bone marrow space (Fig. 1b). Next, TauT antibodies were used to localize TauT expression in the bones (Fig. 2). Tissues from the femurs of

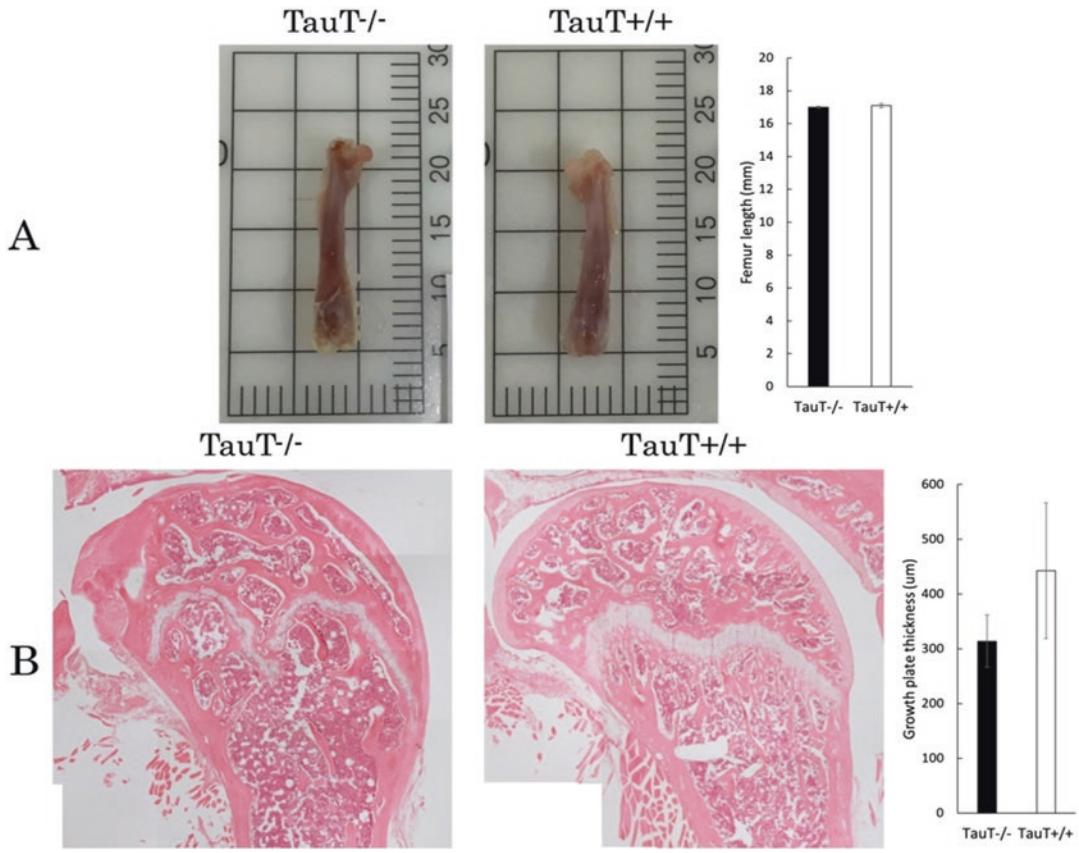

Fig. 1 External morphological and histopathological analyses of the femurs of TauT−/− mice. (**a**) There were no abnormal changes in external appearance of the femurs from the TauT−/− mice, which were similar to those from the TauT+/+ mice. The femur lengths were also not significantly different between the TauT−/− and TauT+/+ mice ($P = 0.563$). (**b**) The specific histological features of the TauT−/− mouse femur were a small number of trabeculae, the thin cortical bone and epiphyseal plate thicknesses, and a wide bone marrow space

TauT−/− and TauT+/+ mice were immunostained using the avidin–biotin complex method. Osteoblasts are normally distributed throughout the surface of a trabecula. Numerous TauT-immunopositive cells were observed in the broad part of the trabecula in all TauT+/+ mice, but not in the TauT−/− mice (Fig. 2). Osteoblasts were observed on the surface of the bone matrix. There was a mixture of cuboidal activated osteoblasts and flattened differentiated osteoblasts in the bone tissue of the TauT+/+ mice, whereas undifferentiated osteoblasts were more frequently observed in that of the TauT−/− mice. Since the thickness of the growth plate affects bone formation, we analyzed the growth plate cartilage in these mice. The ossification zone of the TauT+/+ mouse femur shown in Fig. 1b revealed that the growth plate was of equivalent thickness. By contrast, the growth plate of the TauT−/− mouse femur was of unequal thickness, and some areas were interrupted. However, the difference in growth plate thickness between the TauT−/− and TauT+/+ groups was not statistically significant (314.2 ± 47.8 and 443.0 ± 123.5 μm, respectively; $P = 0.114$).

3.2 Analysis of Bone Mineral Density in TauT−/− Mice

To assess the function of taurine, the BMDs of the TauT−/− and TauT+/+ mice were evaluated

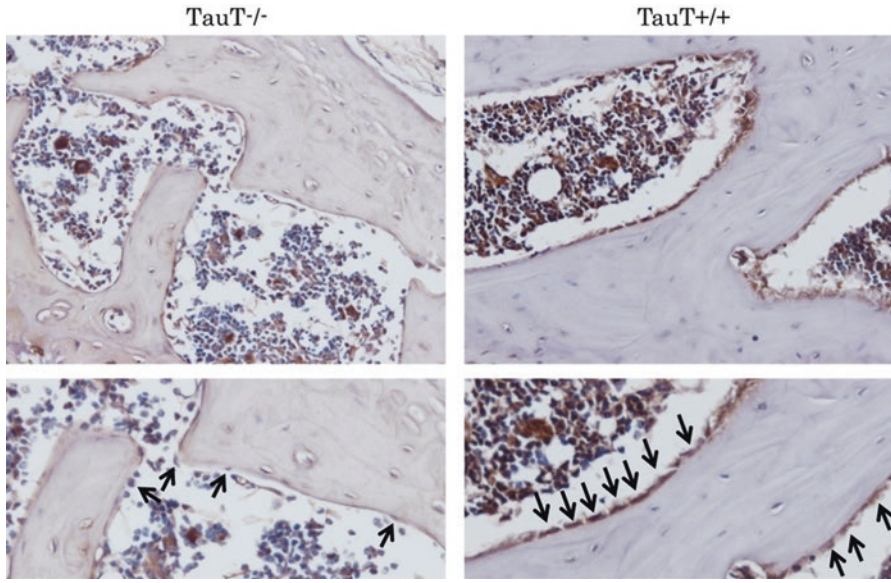

Fig. 2 Localization of taurine transporter (TauT) expression in bone tissue of TauT+/+ and TauT−/− mice. The spatial distributions of taurine and TauT in osteoblasts on the bone surface are shown. Intense TauT immunoreactivity was observed in the osteoblasts of the TauT+/+ mouse femur, whereas weak TauT immunoreactivity was observed in those of the TauT−/− mouse femur

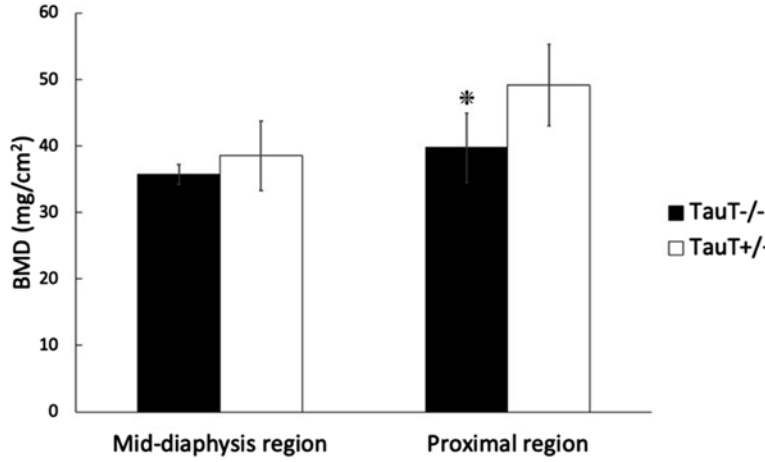

Fig. 3 Comparative analysis of the bone mineral density (BMD) in TauT−/− and TauT+/+ mice. In the mid-diaphysis region, the BMD was not significantly different between the TauT−/− and TauT+/+ groups ($P = 0.261$). In the proximal region, the BMD in the TauT−/− mice was significantly lower ($P = 0.003$)

by DEXA scanning of the proximal and mid-diaphysis regions (Fig. 3). In the mid-diaphysis region (Fig. 3), the BMD of the TauT−/− group was not significantly different from that of the TauT+/+ group (35.7 ± 1.5 and 38.5 ± 5.2 g/cm^2, respectively; $P = 0.261$). By contrast, in the proximal region (Fig. 3), the BMD was significantly lower in the TauT−/− mice than in the TauT+/+ mice (39.7 ± 5.2 and 49.1 ± 6.1 g/cm^2, respectively; $P = 0.003$).

3.3 Structural Analysis of Femoral Trabeculae in TauT−/− Mice Using Micro-computed Tomography

Femurs from the TauT−/− and TauT+/+ mice were analyzed using micro-CT, and the representative 3D reconstructions are shown in Fig. 4a. With regard to the trabecular bone parameters, the BV (0.13 ± 0.03 and 0.18 ± 0.02 mm^3, $P = 0.015$)

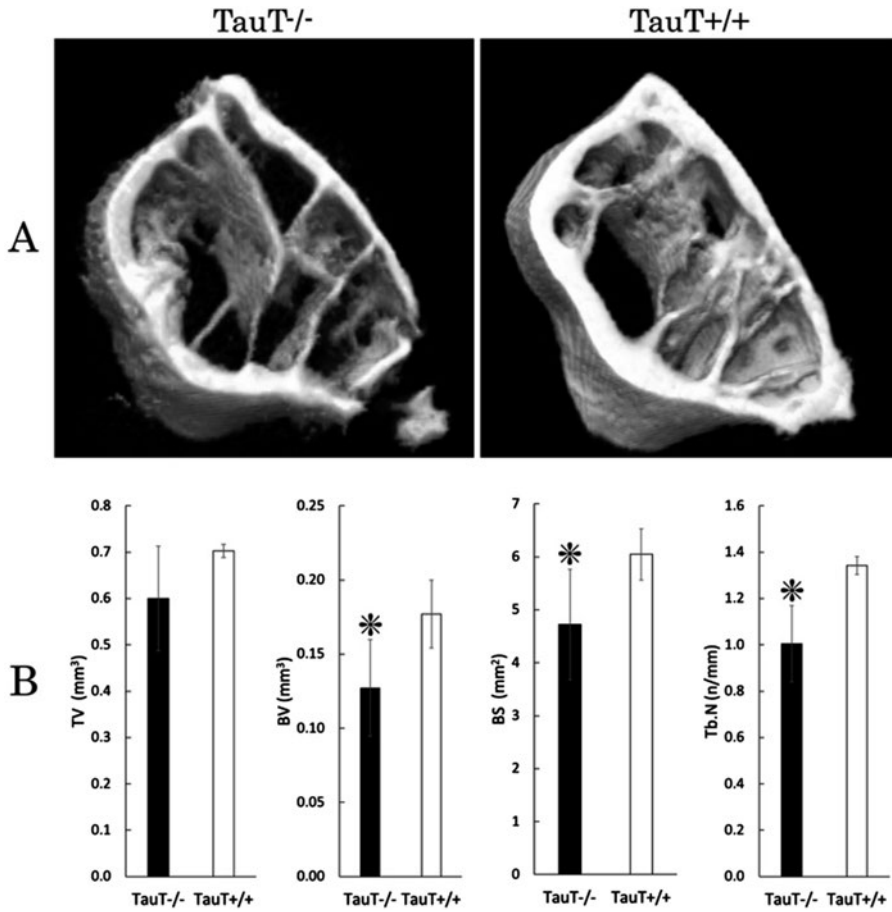

Fig. 4 Structural analysis of femoral trabeculae in TauT−/− mice using micro-CT. The bone microstructure was evaluated in both TauT−/− and TauT+/+ mice. (**a**) Three-dimensional microstructural images of the proximal region of the femurs in both mouse groups. (**b**) The specific micro-CT features of the TauT−/− mouse femur were a significantly smaller bone volume (BV; $P = 0.015$), bone surface (BS; $P = 0.015$), and trabecular number (Tb.N; $P = 0.002$)

and BS values (4.72 ± 1.04 and 6.05 ± 0.48 mm^2, $P = 0.015$) were significantly decreased in the TauT−/− mice relative to the values in the TauT+/+ mice (Fig. 4b). By contrast, there was no significant difference between the two mouse groups in terms of the TV, BV/TV, and BS/TV values. The Tb.N was also significantly lower in the TauT−/− mice (1.00 ± 0.16 n/mm) than in the TauT+/+ mice (1.34 ± 0.04 n/mm). Additionally, no differences in Tb.Th (81.8 ± 14.0 and 80.9 ± 10.9 μm, respectively; $P = 0.146$) and Tb.Sp (175.8 ± 42.5 and 161.9 ± 33.9 μm, respectively; $P = 0.192$) were observed between the TauT−/− and TauT−/− mice.

4 Discussion

In this study, the bone status (e.g., femoral growth plate, BMD, and bone microstructure) in TauT−/− mice was investigated. The results revealed that TauT−/− mice had a lower BMD and poorer bone microstructure than TauT+/+ mice, suggesting that taurine deficiency decreases bone density and quality and therefore increases the risk of fracture. To the best of our knowledge, this is the first study to assess the bone status in TauT−/− mice.

As previously described, TauT, which is also expressed in osteoblasts, maintains a constant

level of taurine in the bone tissue, allowing the amino acid to perform important bone functions and promote osteoblast differentiation. Taurine supplementation has been shown to improve bone formation and differentiation in *ovariectomized* rats (Choi 2017) and in a rabbit model of glucocorticoid-induced osteonecrosis (Hirata et al. 2020). Taurine affects the expression of connective tissue growth factor through cell signaling pathways in osteogenic cells and has been associated with increased ALP activity and collagen synthesis in osteoblast-like UMR-106 cells (Park et al. 2001). It also activates nuclear factor erythroid 2-related factor 2 (Nrf2); induces the expression of the antioxidant enzymes NAD(P)H dehydrogenase [quinone] 1 (NQO1), heme oxygenase 1 (HO1), and glutamate–cysteine ligase catalytic subunit (GCLC); and reduces H_2O_2-induced cell death by activating extracellular signal-regulated kinase (ERK) and the Wnt/β--catenin pathway in osteoblasts. Additionally, the partial reduction in ERK, antioxidant, and ALP activities by a Wnt/β-catenin inhibitor suggests the involvement of other signaling molecules and pathways (Lou et al. 2018). Taurine has been found to mediate the activation of ALP activity and osteocalcin secretion and the inhibition of intracellular reactive oxygen species (Lou et al. 2018). Our findings are consistent with these previous reports. In particular, we found that the TauT−/− mice, which are inherently taurine deficient, had many undifferentiated osteoblasts and a low BMD. Our findings indicate that taurine deficiency may result in osteoblast immaturity and a decrease in the bone density. Considering that oxidative stress is a biomarker of postmenopausal osteoporosis, it is possible that the antioxidative effect of taurine could be involved.

Taurine deficiency leads to poor bone microstructure. Bone strength depends on the intrinsic properties of the materials that take part in bone matrix mineralization, the BMD, and the bone microstructure. The mechanical properties of trabecular bone tissue are determined by the bone microstructure (Fritsch and Hellmich 2007). In normal bone formation, the volume per year turnover rate is 26% for trabecular bone and 3% for cortical bone. Because trabecular bone is more active in remodeling, it is less mineralized than cortical bone (Webster and Jee 1983). The strength of trabecular bone is related to bone fracture and damage, which cause bone remodeling (Lotz et al. 1991). Bone strength is 70% determined by the bone density and 30% by the bone quality (Klibanski et al. 2001). The bone microstructure is the most critical factor for good bone quality. Several reports have been published on the effects of taurine supplementation on the bone microstructure. For example, in vitamin B_{12}-deficient mice, oral taurine administration increased the BV/TV by inducing an increase in insulin growth factor 1 (IGF-1) (Roman-Garcia et al. 2014). Oyster shell powder, which has a high taurine content, increased the femoral BMD, trabecular BV, Tb.Th, and Tb.N in ovariectomized mice, suggesting its potential for the treatment of osteoporosis (Han et al. 2007). By contrast, taurine exposure at the dose of 40 mg/kg bodyweight for 8 weeks was ineffective on the microstructures of both compact and trabecular bone tissues (Martiniakova et al. 2019). In this present study, the decrease in Tb.N in the TauT−/− mouse femur was not consistent with a bigger space between the trabeculae or an increase in Tb.Sp. Collectively, the micro-CT features of the proximal femur of the TauT−/− mouse were a smaller BV, BS, and Tb.N, suggesting that taurine is required for skeletal development of the trabecular bone in mice. The difference from previous studies is that the TauT−/− mice used in this study are unable to take up taurine into the cell. Hence, lifelong taurine deficiency may lead to the degradation of the bone microstructure and a reduction in bone quality.

5 Conclusion

In summary, we found that the bone of TauT−/− mice was characterized by a low BMD and poor bone quality, which decreased the bone strength. These findings support the importance of taurine for bone metabolism. The TauT expressed in osteoblasts ensures the maintenance of a high intracellular taurine concentration, indicating

that taurine can promote osteoblast differentiation during bone formation. Lifelong taurine deficiency may result in the degradation of the bone microstructure and a subsequent reduction in bone quality. Further research is needed to determine the exact role of taurine in the maintenance of bone health.

Acknowledgments This work was supported by the Japan Society for the Promotion of Science (JSPS KAKENHI Grant Number JP20K08120).

References

Baliou S, Kyriakopoulos AM, Goulielmaki M, Panayiotidis MI, Spandidos DA, Zoumpourlis V (2020) Significance of taurine transporter (TauT) in homeostasis and its layers of regulation (review). Mol Med Rep 22(3):2163–2173

Camerino DC, Tricarico D, Pierno S, Desaphy JF, Liantonio A, Pusch M, Burdi R, Camerino C, Fraysse B, De Luca A (2004) Taurine and Skeletal Muscle Disorders. Neurochem Res 29(1):135–142

Choi M-J (2009) Effects of taurine supplementation on bone mineral density in ovariectomized rats fed calcium deficient diet. Nutr Res Pract 3:108–113

Choi M-J (2017) Taurine may modulate bone in cholesterol fed estrogen deficiency-induced rats. Adv Exp Med Biol 975:1093–1102

Fritsch A, Hellmich C (2007) 'Universal' microstructural patterns in cortical and trabecular, extracellular and extravascular bone materials: micromechanics-based prediction of anisotropic elasticity. J Theor Biol 244(4):597–620

Gordon RE, Heller RF, Heller RF (1992) Taurine protection of lungs in hamster models of oxidant injury: a morphologic time study of paraquat and bleomycin treatment. Adv Exp Med Biol 315:319–328

Gupta R, Win T, Bittner S (2005) Taurine analogues: a new class of therapeutics: retrospect and prospects. Curr Med Chem 12(17):2021–2039

Han SY, Lee JR, Kwon YK, Jo MJ, Park SJ, Kim SC, Lee HS, Ku SK (2007) Ostreae Testa prevent ovariectomy-induced bone loss in mice by osteoblast activations. J Ethnopharmacol 114(3):400–405

Hirata H, Ueda S, Ichiseki T, Shimasaki M, Ueda Y, Kaneuji A, Kawahara N (2020) Taurine inhibits glucocorticoid-induced bone mitochondrial injury, preventing osteonecrosis in rabbits and cultured osteocytes. Int J Mol Sci 21(18):6892

Hoffmann EK, Lambert IH, Pedersen SF (2009) Physiology of cell volume regulation in vertebrates. Physiol Rev 89(1):193–277

Huxtable RJ (1992) Physiological actions of taurine. Physiol Rev 72:101–163

Ito T, Kimura Y, Uozumi Y, Takai M, Muraoka S, Matsuda T, Ueki K, Yoshiyama M, Ikawa M, Okabe M, Schaffer SW, Fujio Y, Azuma J (2008) Taurine depletion caused by knocking out the taurine transporter gene leads to cardiomyopathy with cardiac atrophy. J Mol Cell Cardiol 44:927–937

Jeon SH, Lee MY, Kim SJ, Joe SJ, Kim GB, Kim IS, Kim NS, Hong CU, Kim SZ, Kim JS, Kang HS (2007) Taurine increases cell proliferation and generates an increase in [Mg2+]i accompanied by ERK 1/2 activation in human osteoblast cells. FEBS Lett 581:5929–5934

Kato T, Okita S, Wang S, Tsunekawa M, Ma N (2015) The effects of taurine administration against inflammation in heavily exercised skeletal muscle of rats. Adv Exp Med Biol 803:773–784

Klibanski A, Adams-Campbell L, Bassford T, Blair NS (2001) Osteoporosis prevention, diagnosis, and therapy. J Am Med Assoc 285(6):785–795

Lotz JC, Cheal EJ, Hayes WC (1991) Fracture prediction for the proximal femur using finite element models: Part I--Linear analysis. J Biomech Eng 113(4):353–360

Lou J, Han D, Yu H, Yu G, Jin M, Kim SJ (2018) Cytoprotective effect of taurine against hydrogen peroxide-induced oxidative stress in umr-106 cells through the wnt/β-catenin signaling pathway. Biomol Ther 26(6):584–590

Martiniakova M, Sarocka A, Babosova R, Galbavy D, Kapusta E, Goc Z, Formicki G, Omelka R (2019) Bone microstructure of mice after prolonged taurine treatment. Physiol Res 68:519–523

Moon PD, Jeong HJ, Kim HM (2012) Effects of schizandrin on the expression of thymic stromal lymphopoietin in human mast cell line HMC-1. Life Sci 91(11–12):384–388

Park S, Kim H, Kim SJ (2001) Stimulation of ERK2 by taurine with enhanced alkaline phosphatase activity and collagen synthesis in osteoblast-like UMR-106 cells. Biochem Pharmacol 62:1107–1111

Pasantes-Morales H, Cruz C (1985) Taurine: a physiological stabilizer of photoreceptor membranes. Prog Clin Biol Res 179:371–381

Rasgado-Flores H, Mokashi A, Hawkins RA (2012) Na +-dependent transport of taurine is found only on the abluminal membrane of the blood-brain barrier. Exp Neurol 233(1):457–462

Roman-Garcia P, Quiros-Gonzalez I, Mottram L, Lieben L, Sharan K, Wangwiwatsin A, Tubio J, Lewis K, Wilkinson D, Santhanam B, Sarper N, Clare S, Vassiliou GS, Velagapudi VR, Dougan G, Yadav VK (2014) Vitamin B12-dependent taurine synthesis regulates growth and bone mass. J Clin Invest 124:2988–3002

Shigemi K, Tanaka K, Hayamizu K, Denbow DM, Furuse M (2011) L-serine decreases taurine concentration in the extracellular fluid of brain slices. Neurosci Med 2:268–274

Suleiman MS, Moffatt AC, Dihmis WC, Caputo M, Hutter JA, Angelini GD, Bryan AJ (1997) Effect of ischaemia

and reperfusion on the intracellular concentration of taurine and glutamine in the hearts of patients undergoing coronary artery surgery. Biochim Biophys Acta 1324(2):223–231

Warskulat U, Flögel U, Jacoby C, Hartwig HG, Thewissen M, Merx MW, Molojayvi A, Heller-Stilb B, Schrader J, Haussinger D (2004) Taurine transporter knockout depletes muscle taurine levels and results in severe skeletal muscle impairment but leaves cardiac function uncompromised. FASEB J 18:577–579

Webster SJ, Jee S (1983) The skeletal tissues. In: Histology. Elsevier Biomedical Press, Amsterdam, pp 200–254

Yuan LQ, Xie H, Luo XH, Wu XP, Zhou HD, Lu Y, Liao EY (2006) Taurine transporter is expressed in osteoblasts. Amino Acids 31:157–163

Yuan LQ, Lu Y, Luo XH, Xie H, Wu XP, Liao EY (2007) Taurine promotes connective tissue growth factor (CTGF) expression in osteoblasts through the ERK signal pathway. Amino Acids 32:425–430

Yuan LQ, Liu W, Cui RR, Wang D, Meng JC, Xie H, Wu XP, Zhou HD, Lu Y, Liao EY (2010) Taurine inhibits osteoclastogenesis through the taurine transporter. Amino Acids 39:89–99